Dalton Transactions

PAPER

View Article Online
View Journal | View Issue

Cite this: *Dalton Trans.*, 2016, **45**, 10599

Spotlight on the ligand: luminescent cyclometalated Pt(IV) complexes containing a fluorenyl moiety†

Fabio Juliá and Pablo González-Herrero*

Received 2nd May 2016,
Accepted 24th May 2016

DOI: 10.1039/c6dt01722c

www.rsc.org/dalton

The synthesis, electrochemistry and photophysical properties of a family of Pt(IV) complexes with cyclometalated 2-(9,9-dimethylfluoren-2-yl)pyridine (flpy) are reported. Homoleptic and heteroleptic tris-cyclometalated complexes with a meridional configuration, *mer*-[Pt(C^N)$_2$(flpy)]OTf, with C^N = flpy or cyclometalated 2-phenylpyridine (ppy), were prepared by reacting the bis-cyclometalated precursors [Pt(C^N)$_2$Cl$_2$] with flpyH in the presence of two equivalents of AgOTf. The corresponding facial isomers were obtained by photoisomerization. The Pt(IV) complexes with flpy display intense absorptions in the near-visible region and yellow phosphorescence in fluid solutions at 298 K, with quantum yields in the range 0.06–0.28 and lifetimes of hundreds of microseconds. The emissions arise from essentially ^{3}LC (flpy) states in all cases, with little metal-orbital contribution. However, computational calculations and experimental data demonstrate that subtle variations in the contribution of metal orbitals to the emitting state have a profound impact on quantum yields, while nonradiative deactivation through the thermal population of deactivating LMCT states does not have a significant influence.

Introduction

A deep understanding of the behaviour of photoexcited chemical species is crucial for the development of new technologies that take advantage of light as a sustainable source of energy.[1] In this context, the study of the photophysical and photochemical properties of transition metal complexes has been a very active research field for several decades, owing to their versatility and manifold applications. The strong spin–orbit coupling (SOC) induced by second- and third-row transition metal ions enables an efficient population of long-lived triplet excited states *via* rapid intersystem crossing (ISC) from singlet excited states.[2] Such triplet states are highly desirable for important photonic applications, including bioimaging,[3] photocatalysis,[4] photodynamic chemotherapy[5] or the development of electroluminescent devices.[6] In particular, Ru(II),[7] Ir(III)[8] and Pt(II)[9] complexes with heteroaromatic ligands have been extensively studied for their phosphorescence, which generally arises from metal-to-ligand charge transfer (MLCT), ligand-centred (LC) or mixed LC/MLCT excited states. For many of the applications of these transition-metal complexes, high phosphorescence quantum yields (Φ_P) are advantageous, which depend on the quantum yield of intersystem crossing (Φ_{ISC}) and the radiative and nonradiative rate constants of the phosphorescing state (k_r and k_{nr}, respectively), according to the following equation:

$$\Phi_P = \Phi_{ISC}\frac{k_r}{k_r + k_{nr}}$$

In general, the ISC event is very fast in these complexes and Φ_{ISC} usually approaches unity. Thus, the strategies to obtain high Φ_P values are based on increasing k_r and/or reducing k_{nr}.[8a] Phosphorescence is a spin-forbidden transition ($T_n \rightarrow S_0$) and therefore the associated k_r values are generally lower compared to those of fluorescent emissions ($S_n \rightarrow S_0$). However, the SOC induced by heavy transition metals causes a mixing of states of different spin multiplicities, leading to less pure spin states and higher k_r values.[2] Accordingly, a decrease in metal orbital contribution to the emitting excited state, which is usually associated with a lower MLCT character, causes a reduction in k_r.[10] This is especially important in metal complexes that emit from essentially ^{3}LC states, in which obtaining modest k_r values is crucial to achieve significant quantum yields. Alternatively, highly efficient emissions can be obtained by hindering nonradiative processes. Aside from bimolecular quenching, transition metal complexes typically display two main intramolecular nonradiative deactivation channels: thermal population of low-lying quenching states and vibrational coupling to the ground state. The first one involves non-emissive states that are close in energy to the emitting

Departamento de Química Inorgánica, Facultad de Química, Universidad de Murcia, Apdo. 4021, 30071 Murcia, Spain. E-mail: pgh@um.es

† Electronic supplementary information (ESI) available: Additional spectroscopic and computational data. See DOI: 10.1039/c6dt01722c

state. Frequently, these quenching states result from the population of metal dσ* orbitals, *i.e.* metal-centred (MC)[11] or ligand-to-metal charge transfer (LMCT)[12] states, leading to important geometry distortions, dissociation of ligands or even reduction of the metal center.[13] The use of strong-field ligands such as carbenes or cyclometalated scaffolds has proven to raise the energy of these states, thereby reducing quenching.[9b,14] Vibrational coupling to the ground state is especially important in emitting states that lie at low energies or display distorted structures with respect to the ground state. In order to prevent distortions in the excited state, rigid complexes have been prepared by using pincer[15] or tetradentate[16] ligands as well as assembling dendrimeric structures[17] or extending π-conjugation in the ligands.[18] In particular, the use of cyclometalated ligands bearing a fluorenyl instead of a phenyl moiety has been notably successful in improving the emission properties of transition metal complexes. In fact, strongly emissive Ir(III),[11a,19] Pt(II),[20] Pd(II)[21] and Au(III)[22] complexes have been reported with this type of ligands, which show lower k_{nr} values in comparison with the phenyl derivatives in most cases.

Recently, we prepared the first family of meridional (*mer*) and facial (*fac*) homoleptic tris-cyclometalated Pt(IV) complexes *mer*/*fac*-$[Pt(C^N)_3]^+$, with C^N = cyclometalated 2-phenylpyridine (ppy), 2-(*p*-tolyl)pyridine (tpy), 2-(2,4-difluorophenyl) pyridine (dfppy), or 1-phenylpyrazole (ppz); the *fac* isomers display blue emissions from essentially ^{3}LC states with quantum yields up to 0.49 in fluid solution at 298 K and lifetimes of hundreds of microseconds.[23] In order to examine the colour tunability of this class of complexes, we later addressed the introduction of cyclometalated ligands of lower π–π* transition energies and prepared heteroleptic derivatives *mer*-$[Pt(C^N)_2(C'^N')]^+$, with C^N = ppy or dfppy and C'^N' = cyclometalated 2-(2-thienyl)pyridine (thpy) or 1-phenylisoquinoline (piq), which showed yellow or orange phosphorescent emissions arising from ^{3}LC states localized on the thpy or piq ligands, respectively, but lower efficiencies.[24] The attempts to obtain heteroleptic *fac*-$[Pt(C^N)_2(C'^N')]^+$ or homoleptic *mer*-$[Pt(C'^N')_3]^+$ complexes with C'^N' = thpy or piq were unsuccessful because they led to reduction to Pt(II).[24] In the light of these results, we set out to obtain more stable and rigid derivatives using a cyclometalated ligand incorporating a fluorenyl moiety. In a recent article, we reported a family of neutral complexes of the type $[Pt(C^N)_2(Me)Cl]$, including one example with cyclometalated 2-(9,9-dimethylfluoren-2-yl)pyridine (flpy), that displays yellow phosphorescence with a good emission efficiency, long lifetime and high absorptivity.[25] Herein, we present the preparation, photophysical characterization and electrochemistry of homoleptic and heteroleptic tris-cyclometalated complexes containing flpy as the chromophoric ligand, together with a neutral bis-cyclometalated derivative, which display long-lived yellow phosphorescence in all cases and reach quantum yields up to 0.28.

Results and discussion

Synthesis

The synthetic routes to the Pt(IV) complexes with the flpy ligand are outlined in Scheme 1. We first explored the preparation of heteroleptic tris-cyclometalated complexes containing two ppy as supporting ligands and one flpy as the chromophoric ligand by following a similar procedure to that reported for other heteroleptic complexes.[24] Thus, the reaction of

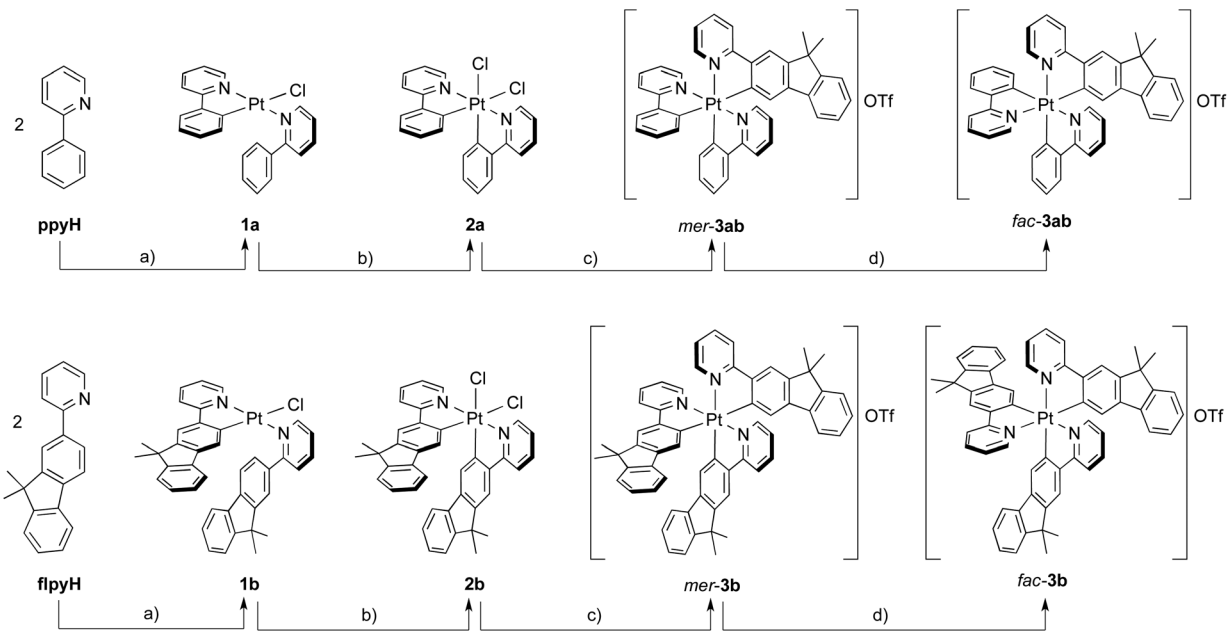

Scheme 1 Synthetic routes to tris-cyclometalated Pt(IV) complexes with flpy. Reagents and conditions: (a) K_2PtCl_4, $EtOCH_2CH_2OH/H_2O$ (3 : 1), 80 °C, 2 days; (b) $PhICl_2$, CH_2Cl_2, 25 °C, 1 h; (c) flpyH, 2 AgOTf, 1,2-dichloroethane, 90 °C, 2 days; (d) *hν*, MeCN, 3 h.

$[Pt(ppy)_2Cl_2]$ (**2a**)[26] with flpyH in the presence of 2 equiv. of AgOTf in 1,2-dichloroethane at 90 °C afforded *mer*-$[Pt(ppy)_2(flpy)]OTf$ (*mer*-**3ab**) in moderate yield. Irradiation of a MeCN solution of the latter satisfactorily resulted in photoisomerization to the facial isomer, *fac*-$[Pt(ppy)_2(flpy)]OTf$ (*fac*-**3ab**). Encouraged by these results, we next addressed the synthesis of homoleptic flpy derivatives using a similar route. The first step required the preparation of [Pt(flpy)(flpyH)Cl] (**1b**) from K_2PtCl_4 by using the procedure reported for other derivatives with ppy-based ligands.[27] Oxidation of this compound with $PhICl_2$ led to the cyclometalation of the pendant (9,9-dimethylfluoren-2-yl) moiety of the flpyH ligand and the introduction of a second chloride to give $[Pt(flpy)_2Cl_2]$ (**2b**) in nearly quantitative yield. The introduction of the third flpy ligand to give *mer*-$[Pt(flpy)_3]OTf$ (*mer*-**3b**) and the subsequent photoisomerization to *fac*-$[Pt(flpy)_3]OTf$ (*fac*-**3b**) succeeded following the method employed for the heteroleptic derivatives. Complexes *fac*-**3ab** and *mer*/*fac*-**3b** are the first *fac*-heteroleptic and *mer*/*fac*-homoleptic tris-cyclometalated Pt(IV) complexes bearing a cyclometalated ligand of a relatively low π–π* transition energy. Their successful synthesis contrasts with the results obtained previously with thpy and piq ligands.

Photophysical properties

The absorption spectra of complexes **2b**, *mer*/*fac*-**3ab** and *mer*/*fac*-**3b** were recorded in CH_2Cl_2 (*ca.* 1×10^{-5} M) at 298 K (Fig. 1, Table 1). All complexes give rise to intense and structured absorptions in the range of 250–400 nm that can be ascribed predominantly to ^{1}LC (π–π*) transitions within the cyclometalated ligands. The lowest-energy band is very similar in shape and energy in all derivatives, which indicates that it arises from the flpy ligand; this is further supported by the fact that its molar absorptivity increases with the number of flpy ligands and can reach 70 000 M^{-1} cm^{-1}; such highly intense absorptions in the near-visible range are particularly desirable for applications in the fields of photocatalysis or bioimaging. The heteroleptic complexes *mer*-**3ab** and *fac*-**3ab** exhibit additional bands in the range 310–350 nm. Thus, the facial isomer shows structured bands in the range 310–335 nm that resemble those of *fac*-$[Pt(ppy)_3]OTf$, which arise from π–π* transitions within the ppy ligands; the same assignment is plausible for these absorptions in *fac*-**3ab**. The absorption spectrum of *mer*-**3ab** displays a broad band centred at ~350 nm, probably resulting from mixed LLCT/LC(ppy) transitions. These assignments are in agreement with the results obtained by TDDFT calculations (see the ESI†).

The excitation and emission spectra of complexes **2b**, *mer*/*fac*-**3ab** and *mer*/*fac*-**3b** were registered in CH_2Cl_2 solution at 298 K and in butyronitrile (PrCN) frozen glasses at 77 K. The emission data are summarized in Table 2 and emission spectra at 298 K are depicted in Fig. 1. Excitation spectra at 298 K and emission spectra at 77 K are given in the ESI† (Fig. S7 and S8†). All the studied compounds are luminescent in fluid solution at 298 K, displaying the same structured emission band, with small variations in energy, and radiative lifetimes in the order of hundreds of microseconds. The corresponding excitation spectra match the absorption profiles in all cases (Fig. S10, ESI†), thus confirming that the emissions do not arise from possible photodecomposition products. This is especially significant in the case of *mer*-**3b** because the emissions of all the previously reported *mer* isomers of homoleptic tris-cyclometalated Pt(IV) complexes in fluid solutions were found to arise from small amounts of the photochemically generated *fac* counterparts.[23,24] At 77 K, the emissions are slightly blue-shifted, indicating a very small rigidochromic effect, and their structure becomes better resolved. In addition, lifetimes increase as a result of the partial suppression of nonradiative processes. These features are indicative of

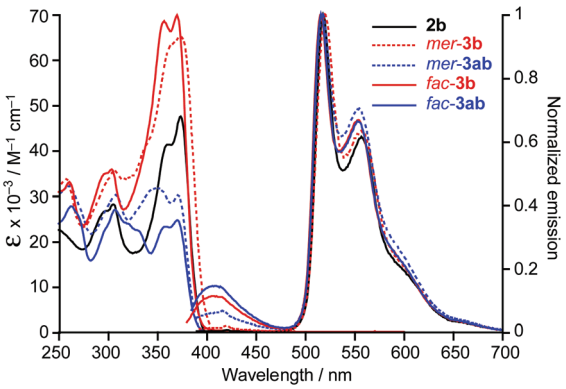

Fig. 1 Absorption and emission spectra of the studied compounds in CH_2Cl_2 at 298 K.

Table 1 Electronic absorption data for the studied complexes in CH_2Cl_2 solution (*ca.* 1×10^{-5} M) at 298 K

Complex	λ/nm (ε × 10^{-3}/M^{-1} cm^{-1})
mer-**3ab**	260 (32.2), 307 (30.2), 348 (31.8), 371 (30.2)
fac-**3ab**	262 (27.9), 306 (27.0), 319 (24.0), 331 (22.5, sh), 356 (23.1, sh), 370 (24.8)
2b	251 (22.5, sh), 297 (26.8, sh), 305 (28.1), 360 (41.2, sh), 373 (47.3)
mer-**3b**	257 (33.7), 305 (35.6), 362 (62.6, sh), 374 (65.0)
fac-**3b**	261 (33.1), 295 (34.8, sh), 303 (35.6), 356 (68.5), 369 (70.0)

Table 2 Emission data of the studied compounds

	298 K[a]					77 K[b]	
Complex	λ_{em}[c]/nm	Φ[d]	τ[e]/μs	k_r[f] × 10^{-3}/s^{-1}	k_{nr}[g] × 10^{-3}/s^{-1}	λ_{em}[c]/nm	τ[e]/μs
mer-**3ab**	517	0.06	252	0.24	3.73	508	1152
fac-**3ab**	516	0.13	218	0.60	3.99	507	708
2b	518	0.28	231	1.21	3.12	510	504
mer-**3b**	520	0.08	154	0.52	5.97	511	660
fac-**3b**	516	0.17	209	0.81	3.97	507	667

[a] In CH_2Cl_2. [b] In PrCN. [c] Highest-energy emission peak. [d] Absolute quantum yield. [e] Emission lifetime. [f] Radiative rate constant, $k_r = \Phi/\tau$. [g] Nonradiative rate constant, $k_{nr} = (1 - \Phi)/\tau$.

an emitting triplet excited state largely centred on the flpy ligand(s) in all cases. Consequently, in the heteroleptic complexes *mer*/*fac*-**3ab** the cyclometalated ppy ligands do not participate in the emission, thus acting as *ancillary* ligands, because ^{3}LC(ppy) states are expected to lie at higher energies relative to the emitting ^{3}LC(flpy) states. Similar results were found previously for heteroleptic tris-cyclometalated derivatives with thpy and piq ligands.[24] The emission spectra of *fac*-**3b** and *mer*/*fac*-**3ab** show an additional band at a higher energy (407 nm), with a much lower intensity in comparison with the phosphorescent emission, that can be assigned to residual fluorescence in view of its very short lifetime (<0.2 ns) and the excitation spectra registered at its maximum, which match those corresponding to the phosphorescent emission (Fig. S9, ESI†). We have previously observed residual fluorescence in other Pt(IV) complexes with low-energy ^{3}LC states,[24] which implies that the ISC event does not have unit efficiency. Notwithstanding the low intensity of this band together with its extremely short lifetime indicates that Φ_{ISC} is very close to unity (>0.99; see the ESI† for more details) and leads to a very efficient population of the triplet manifold.

The quantum yields of *mer*-**3ab** (0.06) and *mer*-**3b** (0.08) are comparable to those of the previously reported *mer*-$[Pt(ppy)_2(C'^\wedge N')]^+$ complexes (C'^N' = thpy, piq; range 0.02–0.07).[24] As expected, the *fac* counterparts are more efficient emitters, with quantum yields of 0.17 (*fac*-**3b**) or 0.13 (*fac*-**3ab**). For its part, compound **2b** shows the highest quantum yield among the complexes studied in this work (0.28). The measured quantum yields can be interpreted by analysing the radiative and nonradiative rate constants (k_r and k_{nr}, respectively), which have been calculated assuming that Φ_{ISC} = 1, since this approximation has only a marginal influence on the final values (see the ESI† for more details). The k_{nr} values are small and generally lower than those found for the previously reported tris-cyclometalated Pt(IV) complexes with ligands of low π–π* transition energies.[24] The rigid scaffold of the flpy ligand may contribute to reduce nonradiative processes, as previously observed for Au(III) and Pt(II) complexes with cyclometalated ligands bearing the fluorenyl moiety.[20,22] In fact, the structure of the emission band shows that the intensity of the 0–0 transition is significantly higher than that of the vibrational peaks, indicating that geometrical distortions in the excited state with respect to the ground state are small.[28] In the case of *mer*-**3b**, k_{nr} is slightly higher compared with the rest of derivatives, but still allows a moderately intense emission, which contrasts with the behaviour of the homoleptic blue emitters *mer*-$[Pt(C^\wedge N)_3]^+$, whose emissions are intense at 77 K but are totally quenched at room temperature because deactivating LMCT states are thermally populated from the emitting state.[23] Reasonably, the possible quenching excited state in *mer*-**3b** is not efficiently populated because of the low energy of the ^{3}LC(flpy) emitting state. In general, k_r values are very low, suggesting a very low metal orbital involvement in the excited state. Nevertheless, a small degree of MLCT character must be assumed, because it is crucial to produce efficient phosphorescence in largely ^{3}LC emitters. As a matter of fact, complex **2b** shows the highest quantum yield of the studied series, mainly because of its significantly higher k_r, which can be attributed to a higher contribution of metal orbitals to the HOMO as a consequence of its uncharged nature and hence an emitting state with a higher degree of MLCT character. The higher quantum yields of *fac*-**3ab** and *fac*-**3b** compared to the *mer* isomers are also attributable to higher k_r values, which indicate that the *fac* geometry leads to a higher metal orbital involvement in the emitting state, as we have noted in a previous study.[24] Hence, the observed differences in Φ_P in the present series of complexes are mainly dictated by k_r, while nonradiative processes are less important.

Electrochemistry

The electrochemical properties of tris-cyclometalated compounds **3** were investigated using cyclic voltammetry in MeCN solution. The potentials of the most important redox processes and HOMO/LUMO energy estimations are listed in Table 3, and voltammograms covering the full solvent window (from 2.2 to −2.7 V *vs.* SCE) are depicted in Fig. 2. The voltammograms of the heteroleptic *mer*/*fac*-**3ab** complexes are very similar to those of the respective homoleptic *mer*/*fac*-**3b** complexes, suggesting that the frontier orbitals are mainly localized on the flpy ligands in all cases, while the participation of the ppy ligands of *mer*/*fac*-**3ab** might be negligible. In contrast, there are significant differences between *mer* and *fac* isomers. One (*fac* isomers) or two (*mer* isomers) irreversible oxidations are observed within the solvent window. The first oxidation peak in the *mer* complexes is found at less positive potentials (1.53 and 1.57 V *vs.* SCE) compared with the *fac* isomers (1.77 and 1.71 V *vs.* SCE), which is a common behaviour observed for other tris-cyclometalated Pt(IV) derivatives,[23,24] and implies a higher energy of the HOMO in the *mer* isomers. As expected, the potentials of the oxidation processes in the present compounds are much lower than those found for *mer*/*fac*-$[Pt(ppy)_3]$OTf, because the more extended π-conjugation of the fluorenyl system implies an easier oxidation. Several reduction processes are observed before the solvent discharge limit. The first two

Table 3 Electrochemical data[a] and HOMO/LUMO energy estimations[b] for complexes **3**

Complex	E_{pa} [c]	E_{pc} [d]	$E_{1/2}$ [e]	E_{HOMO}	E_{LUMO}	$\Delta E_{HOMO-LUMO}$
mer-**3b**	1.53 2.00	−1.57	−2.22	−6.12	−3.23	2.89
mer-**3ab**	1.57 2.02	−1.55	−2.34	−6.16	−3.26	2.90
fac-**3b**	1.77	−1.73 −1.87	−2.23	−6.28	−3.13	3.15
fac-**3ab**	1.71	−1.78 −1.90	−2.36	−6.27	−3.08	3.19

[a] In V relative to SCE, measured in 0.1 M $(Bu_4N)PF_6$ anhydrous MeCN solution at 100 mV s^{-1}. [b] In eV; estimated from the onset values of the oxidation and reduction waves referenced against Fc^+/Fc (0.40 V *vs.* SCE in MeCN), using a formal potential of 5.1 eV for the Fc^+/Fc couple in the Fermi scale.[39] [c] Irreversible anodic peak potential. [d] Irreversible cathodic peak potential. [e] For the reversible process.

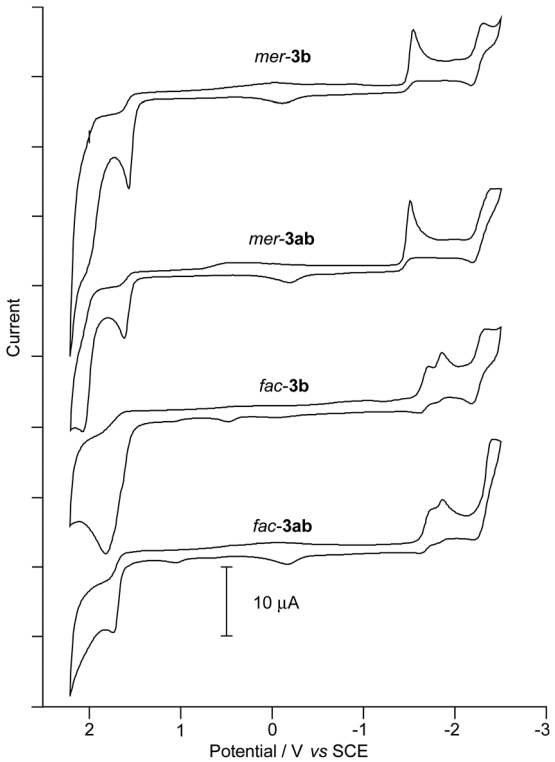

Fig. 2 Cyclic voltammograms of compounds **3** in MeCN at 100 mV s^{-1}.

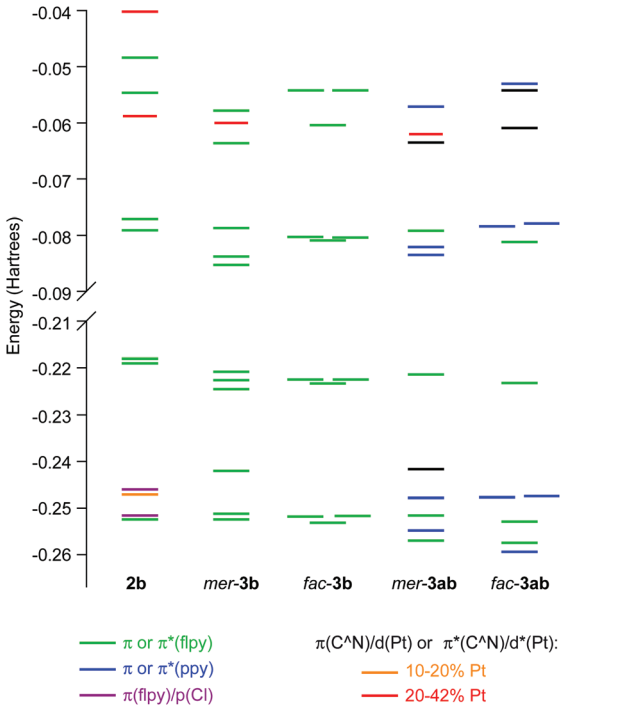

Fig. 3 Orbital energy diagrams from DFT calculations for **2b**, *mer*/*fac*-**3b** and *mer*/*fac*-**3ab**.

reduction peaks found for the *fac* complexes are irreversible and occur at very close potentials (from −1.73 to −1.90 V *vs.* SCE); they probably arise from the consecutive reductions of two cyclometalated ligands. The first reduction in the *mer* compounds is also irreversible, but occurs at less negative potentials (−1.57 and −1.55 V *vs.* SCE) and is not followed by another close-lying peak. At more negative potentials, a reversible or quasi-reversible wave is observed in all cases, probably arising from the reduction and reoxidation of cyclometalated Pt(II) compounds formed in the previous reductions of Pt(IV) species, as proposed in the electrochemical studies of other tris-cyclometalated derivatives.[24]

DFT and TDDFT calculations

For a better understanding of the excited states of the studied compounds, DFT and TDDFT calculations were carried out for all of them at the B3LYP/(6-31G**+LANL2DZ) level including solvent effects (CH_2Cl_2) at the PCM level. The bond distances and angles around the metal in the optimized ground-state geometries (Table S17; ESI†) are in good agreement with the expected values in view of previously reported crystal structures of complexes of the types $[Pt(C^N)_2Cl_2]$[29] and *mer*-$[Pt(C^N)_3]^+$.[23,24] A diagram representing the energies and composition of the frontier orbitals of the optimized ground-state geometries is depicted in Fig. 3. Detailed compositions and figures showing the topologies of these orbitals are given in the ESI.† In general, the frontier orbitals are mainly composed of π or π* orbitals of cyclometalated ligands with some contribution of metal orbitals. It can be observed that, while π* orbitals of both ppy and flpy lie at similar energies, π orbitals of flpy lie at significantly higher energies relative to those of ppy, which is consistent with the above discussed electrochemical data. As a result, the HOMO is essentially a π(flpy) orbital in all cases, involving very little metal character. Nevertheless, a higher metal orbital contribution to the HOMO can still be discerned for **2b** (*ca.* 2%) with respect to *mer*/*fac*-**3ab** and *mer*/*fac*-**3ab** (*ca.* 1%), associated with its uncharged nature, which results in higher energy of the occupied d(Pt) orbitals. Consistent with this, the HOMO−3 in **2b** involves 12% of metal orbital contribution, while in the cationic compounds the first occupied orbitals with metal contributions higher than 10% are HOMO−9 (*mer*/*fac*-**3ab**) and HOMO-13 (*mer*/*fac*-**3b**). Unoccupied orbitals with significant dσ*(Pt) orbital contributions lie at much higher energies in the *fac* derivatives in comparison with their *mer* isomers, which indicates that the *fac* geometry leads to a larger ligand-field splitting. Besides, narrower HOMO–LUMO gaps are found in the *mer* isomers as a result of a lower LUMO and a higher HOMO, in line with the electrochemical results.

Singlet and triplet excitation energies were calculated at the optimized ground-state geometries by TDDFT in CH_2Cl_2 solution. Listings of selected excitations with their assignments and the estimated percentage of MLCT or LMCT character are given in the ESI.† The calculated singlet excitations are in good agreement with the experimental absorption spectra in all cases and confirm that π–π* transitions within the flpy ligand are the main contribution to the lowest-energy band. In

addition, LLCT transitions also contribute to the absorption profiles of *mer*-**3b** and *mer*/*fac*-**3ab** as a result of the presence of inequivalent ligands. LMCT contributions are important in the lowest singlet states of *mer*-**3a** and *mer*-**3ab** because of the relatively low energies of unoccupied orbitals with a high dσ* (Pt) character, while they are negligible in the *fac* isomers. The presence of excited states with a significant LMCT character has been noted for other tris-cyclometalated Pt(IV) complexes with a *mer* configuration and proposed to be responsible for the *mer*-to-*fac* photoisomerization.[23,24]

The TDDFT calculations predict *n* low-lying triplet excitations of the essentially ^{3}LC character ($^3\pi$–π^*) (Fig. 4), where *n* is the number of cyclometalated ligands, each one confined within a different ligand. In all cases the lowest-energy triplet excitation corresponds to a ^{3}LC(flpy) transition, which has a similar energy in all derivatives (2.47–2.52 eV), in agreement with the very similar emission energies. ^{3}LC(ppy) excitations in complexes *mer*/*fac*-**3ab** are considerably higher in energy than the ^{3}LC(flpy) ones, in line with the scenario observed in the frontier-orbital analysis. Hence, the ppy ligands are not expected to participate in the emitting state, thus acting as *non-chromophoric* or *ancillary* ligands in these complexes. Triplet excitations with a LMCT character higher than 10% are in the range 3.46–3.69 eV for **2b**, *mer*-**3b** and *mer*-**3ab**, while analogous transitions are not found below 4.10 or 4.37 eV for *fac*-**3b** or *fac*-**3ab**, respectively, as a consequence of the high energy of their dσ*(Pt) orbitals. Nevertheless, the energy difference between the ^{3}LMCT states and the lowest ^{3}LC(flpy) state appears to be too high to efficiently quench the phosphorescence in all cases, allowing moderate emission intensities even in *mer*-**3b**, as anticipated in the Photophysical properties section.

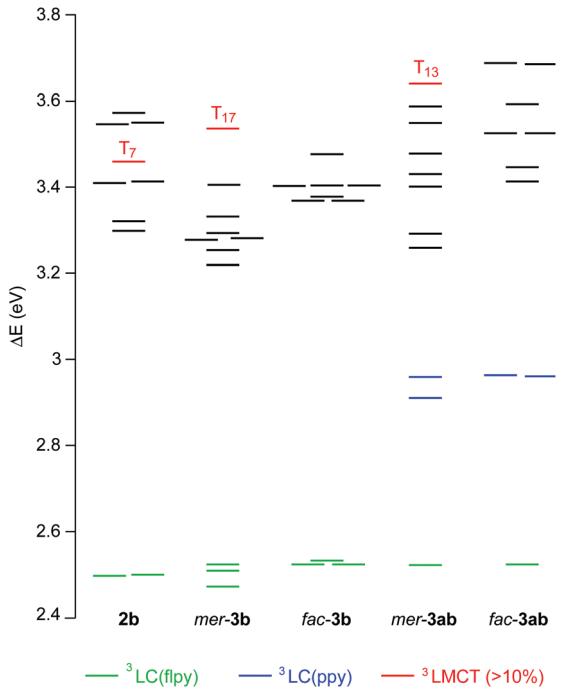

Fig. 4 Energy diagram showing the lowest triplet vertical excitations of **2b**, *mer*/*fac*-**3b** and *mer*/*fac*-**3ab** at the ground-state geometries.

To gain further insight into the nature of the emitting states, we optimized the geometries of the first triplet excited state of the studied complexes. The calculated electronic energies relative to the ground state (adiabatic energy differences) are 2.41 eV (**2b**; 515 nm) or 2.43 eV (rest of complexes; 510 nm), in good agreement with the experimental emission energies. The spin density isosurfaces of the optimized T_1 states (Fig. 5) correspond to π–π* excitations primarily localized within an flpy ligand with little metal-orbital participation in all cases, which is in line with the observation of residual fluorescence in the emission spectra. Nonetheless, a simple visual inspection reveals a higher spin density on the metal in the lowest triplet of the neutral complex **2b** with respect to the cationic derivatives, which implies a higher metal-orbital participation in the emitting state and a higher MLCT character; analogously, among the studied tris-cyclometalated complexes, a higher spin density on the metal is observed for the lowest triplet of the *fac* isomers relative to the *mer* isomers. The calculated natural spin densities on the Pt atom agree with these observations, decreasing in the sequence: **2b** (0.0116) > *fac*-**3ab** (0.0093) ≈ *fac*-**3b** (0.0092) > *mer*-**3b** (0.0044) ≈ *mer*-**3ab** (0.0043). Thus, they follow the same trend observed experimentally for k_r and can be regarded as a reliable indication of the degree of MLCT admixture in the essentially ^{3}LC emitting states. It is also noteworthy that variations in these small MLCT admixtures have a profound

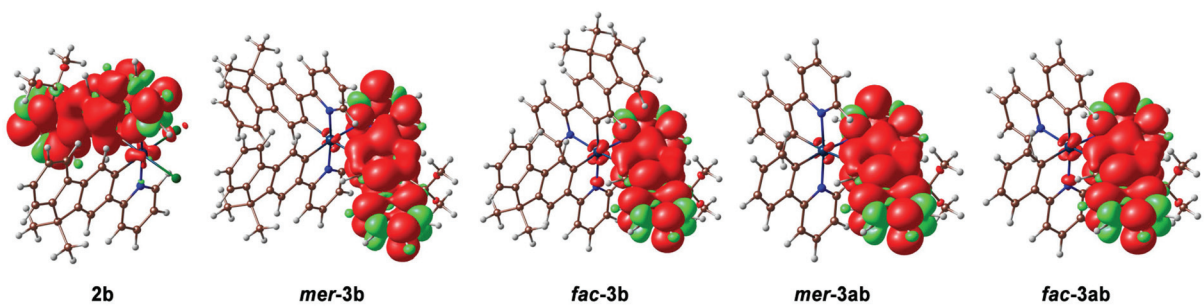

Fig. 5 Spin density distributions (0.001 e bohr^{-3}) for the lowest triplet excited state of the studied compounds.

impact on the emission properties and explain the different emission quantum yields observed for the complexes presented in this work.

Conclusions

A series of luminescent cyclometalated Pt(IV) complexes with the flpy ligand, comprising $[Pt(flpy)_2Cl_2]$, *mer*/*fac*-$[Pt(ppy)_2(flpy)]OTf$ and *mer*/*fac*-$[Pt(flpy)_3]OTf$, have been synthesized and their photophysical properties analysed with the help of DFT and TDDFT calculations. The electrochemical characterization of the tris-cyclometalated derivatives has also been carried out. Notably, complexes *fac*-$[Pt(ppy)_2(flpy)]OTf$ and *mer*/*fac*-$[Pt(flpy)_3]OTf$ are the first *fac*-heteroleptic and *mer*/*fac*-homoleptic tris-cyclometalated Pt(IV) complexes containing a cyclometalated ligand of a relatively low π–π* transition energy. All the studied compounds present strong ^{1}LC(flpy) absorptions in the near-visible region and display yellow phosphorescence from predominantly ^{3}LC(flpy) states with quantum yields up to 0.28. The case of *mer*-$[Pt(flpy)_3]OTf$ is especially significant, because it represents the first homoleptic tris-cyclometalated Pt(IV) complex with a *mer* configuration that exhibits phosphorescence in fluid solutions at room temperature, which is a consequence of an inefficient population of deactivating LMCT states owing to the low energy of the emitting ^{3}LC(flpy) state. The metal-orbital contribution to the emitting state has been identified as the main factor determining the radiative rates and quantum yields of the studied complexes, while nonradiative deactivation becomes secondary. Hence, the strategy of minimizing nonradiative processes in low-energy Pt(IV) emitters by using a more rigid chromophoric ligand has been successfully applied, providing important insight that may be used for the rational design of new Pt(IV)-based emitters.

Experimental section

General considerations and materials

Unless otherwise noted, preparations were carried out under atmospheric conditions. Synthesis grade solvents were obtained from commercial sources. Compounds **2a**,[26] flpyH,[30] and $PhICl_2$ [31] were prepared following published procedures. All other reagents were obtained from commercial sources and used without further purification. NMR spectra were recorded on Bruker Avance 300 or 400 spectrometers at 298 K. Chemical shifts are referred to residual signals of non-deuterated solvent. The number of solvation water molecules was calculated from the integral of the ^{1}H NMR water signal, taking into account the water content of the solvent blank. Elemental analyses were carried out with Carlo Erba 1106 and LECO CHNS-932 microanalyzers. Photoisomerizations were carried out using a UV-Consulting Peschl photoreactor, model UV-RS-1, equipped with a 150 W medium-pressure mercury immersion UV lamp (TQ 150), a quartz cooling jacket, and a 400 mL reaction vessel with a magnetic circulation pump.

Photophysical characterization

UV-vis absorption spectra were recorded on a Perkin-Elmer Lambda 750S spectrophotometer. Excitation and emission spectra were recorded on a Jobin Yvon Fluorolog 3-22 spectrofluorometer with a 450 W xenon lamp, double-grating monochromators, and a TBX-04 photomultiplier. Measurements were carried out in a right angle configuration using 10 mm quartz fluorescence cells for solutions at 298 K or 5 mm quartz NMR tubes for frozen glasses at 77 K. A liquid nitrogen Dewar with quartz windows was employed for low-temperature measurements. Solutions of the samples were degassed by bubbling argon for 30 min; those of *mer*-**3b** and *mer*-**3ab** were degassed in the dark to prevent partial photoisomerization. Lifetimes were measured using the Fluorolog's FL-1040 phosphorimeter accessory; the estimated uncertainty is ±10% or better. Emission quantum yields were measured using a Hamamatsu C11347 Absolute PL Quantum Yield Spectrometer; the estimated uncertainty is ±5% or better.

Electrochemical characterization

Cyclic voltammograms were registered with a potentiostat/galvanostat AUTOLAB-100 (Echo-Chemie, Utrecht), employing a three-electrode electrochemical cell equipped with a glassy carbon working electrode (Metrohm, 2 mm diameter), an Ag/AgCl/3 M KCl electrode reference, and a glassy carbon rod counter electrode. The measurements were carried out at 298 K under an argon atmosphere, using degassed 0.5 mM solutions of the complexes in extra-dry MeCN (Acros Organics) and 0.1 M $(Bu_4N)PF_6$ as the electrolyte. Prior to each experiment, the working electrode was polished with an alumina slurry (0.05 μm) and rinsed with water and acetone. The electrodes were activated electrochemically in the background solution by means of several voltammetric cycles at 1 V s^{-1} between −2.7 V and 2.2 V. At the end of each experiment, the reference electrode was checked against the ferrocene/ferricinium redox couple. Potentials are given *vs.* the standard calomel electrode (SCE).

Synthesis of [Pt(flpy)(flpyH)Cl] (1b)

A Carius tube was charged with K_2PtCl_4 (675 mg, 1.62 mmol), flpyH (1.1 g, 4.05 mmol) and a degassed 3 : 1 mixture of 2-ethoxyethanol/water (30 mL) under a N_2 atmosphere and the mixture was stirred at 80 °C for 2 days. Solvents were removed under reduced pressure, the residue was treated with CH_2Cl_2 (40 mL) and stirred with anhydrous $MgSO_4$. The suspension was filtered and the filtrate was concentrated to 10 mL. Upon addition of MeOH (100 mL) a yellow solid precipitated, which was collected by filtration, washed with MeOH (10 mL) and vacuum-dried to give **1b**·H_2O. Yield: 555 mg, 44%. ^{1}H NMR (300.1 MHz, CD_2Cl_2): δ 9.61 (dd with satellites, J_{HH} = 5.8, 1.3 Hz, J_{HPt} ~39 Hz, 1H), 9.25 (dd with satellites, J_{HH} = 5.8, 1.4 Hz, J_{HPt} ~43 Hz, 1H), 8.63 (d, J_{HH} = 1.2 Hz, 1H), 8.10 (td, J_{HH} = 8.0, 1.6 Hz, 1H), 7.84 (m, 2H), 7.74 (m, 1H), 7.64–7.55 (m, 3H), 7.48

(ddd, J_{HH} = 5.9, 1.7, 1.5 Hz, 1H), 7.42–7.21 (m, 8H), 7.06 (ddd, J_{HH} = 5.9, 1.6, 1.4 Hz, 1H), 6.46 (s with satellites, J_{HPt} ~49 Hz, 1H), 1.41 (s, 3H), 1.38 (s, 3H), 1.29 (s, 3H), 1.16 (s, 3H). $^{13}C\{^1H\}$ NMR (75.45 MHz, CD_2Cl_2): δ 162.9 (C), 154.9 (CH), 154.5 (C), 153.1 (C), 151.2 (CH), 148.8 (C), 140.5 (C), 140.2 (C), 139.4 (C), 139.1 (C), 138.7 (CH), 138.3 (CH), 128.4 (CH), 128.0 (CH), 127.8 (CH), 127.3 (CH), 127.1 (CH), 125.5 (CH), 124.1 (CH), 123.0 (CH), 122.1 (CH), 121.6 (CH), 120.6 (CH), 120.0 (CH), 119.5 (CH), 118.4 (CH), 117.8 (CH), 47.2 (C), 46.7 (C), 27.3 (CH_3), 27.1 (CH_3), 26.8 (CH_3), 26.3 (CH_3). Elemental analysis calcd for $C_{40}H_{35}ClN_2OPt$: C, 60.79; H, 4.46; N, 3.54; found: C, 60.70; H, 4.41; N, 3.59.

Synthesis of [Pt(flpy)$_2$Cl$_2$] (2b)

To a solution of **1b** (370 mg, 0.479 mmol) in CH_2Cl_2 (60 mL) was added $PhICl_2$ (150 mg, 0.545 mmol) and the mixture was stirred at room temperature for 4 h. The resulting suspension was concentrated under reduced pressure (30 mL) and Et_2O (70 mL) was added. The resultant beige precipitate was filtered off, washed with Et_2O (2 × 5 mL) and vacuum-dried to give **2b**·0.5CH_2Cl_2. Yield: 375 mg, 97%. ^1H NMR (400.9 MHz, dmso-d_6): δ 9.75 (dd with satellites, J_{HH} = 6.0, 1.0 Hz, J_{HPt} = 28 Hz, 2H), 8.61 (m, 2H), 8.45 (td, J_{HH} = 7.6, 1.4 Hz, 2H), 8.28 (s, 2H), 7.83 (m, 2H), 7.48 (d, J_{HH} = 7.4 Hz, 2H), 7.31–7.20 (m, 6H), 6.24 (s with satellites, J_{HPt} = 34 Hz, 2H), 1.44 (s, 6H), 1.36 (s, 6H). $^{13}C\{^1H\}$ NMR (100.9 MHz, dmso-d_6): δ 163.5 (C), 154.2 (C), 150.8 (C), 148.8 (CH), 141.9 (CH), 141.3 (C), 140.5 (C), 139.3 (C), 136.7 (C), 128.5 (CH), 127.2 (CH), 124.6 (CH), 123.0 (CH), 121.7 (CH), 120.8 (CH), 120.2 (CH), 117.4 (CH), 46.2 (C), 26.9 (CH_3), 26.3 (CH_3). Elemental analysis calcd for $C_{40.5}H_{33}Cl_3N_2Pt$: C, 57.28; H, 3.92; N, 3.30; found: C, 57.49; H, 4.02; N, 3.54.

Synthesis of *mer*-[Pt(C^N)$_2$(flpy)]OTf

A Carius tube was charged with complex **2a** or **2b** (0.266 mmol), AgOTf (0.585 mmol), flpyH (1.27 mmol) and degassed 1,2-dichloroethane (20 mL) under a N_2 atmosphere, and the mixture was stirred at 90 °C for 2 days. After cooling to room temperature, CH_2Cl_2 (15 mL) was added and the suspension was filtered through Celite. The filtrate was stirred vigorously with Na_2CO_3, filtered and concentrated under reduced pressure (15 mL). Upon addition of Et_2O (60 mL), a solid precipitated, which was filtered off, washed with Et_2O (2 × 5 mL) and vacuum-dried.

***mer*-3ab.** This product was purified by chromatography on silica gel using a $CHCl_3$/MeOH mixture (9 : 1) as the eluent. Beige solid. Yield: 57%. ^1H NMR (400.9 MHz, CD_2Cl_2): δ 8.31 (d, J_{HH} = 8.2 Hz, 1H), 8.18–8.01 (m, 7H), 7.94–7.85 (m, 3H), 7.59 (ddd with satellites, J_{HH} = 6.1, 1.4, 0.7 Hz, J_{HPt} = 30 Hz, 1H), 7.45 (d, J_{HH} = 7.5 Hz, 1H), 7.40–7.12 (m, 10H), 7.04 (s with satellites, J_{HPt} = 21 Hz, 1H), 6.49 (dd with satellites, J_{HH} = 7.3, 0.9 Hz, J_{HPt} = 14 Hz, 1H), 6.24 (dd with satellites, J_{HH} = 7.8, 0.8 Hz, J_{HPt} = 30 Hz, 1H), 1.57 (s, 3H), 1.47 (s, 3H). $^{13}C\{^1H\}$ NMR (75.45 MHz, CD_2Cl_2): δ 167.9 (C), 166.0 (C), 164.4 (C), 161.6 (C), 161.0 (C), 155.0 (C), 152.4 (C), 150.2 (J_{CPt} = 17 Hz, CH), 148.7 (CH), 146.2 (CH), 143.7 (C), 143.1 (C), 142.5 (C), 142.0 (C), 141.9 (CH), 141.5 (CH), 140.7 (CH), 140.2 (C), 138.5 (C), 133.0 (CH), 132.9 (J_{CPt} = 40 Hz, CH), 130.6 (J_{CPt} = 24 Hz, CH), 128.6 (CH), 127.3 (CH), 127.2 (J_{CPt} = 30 Hz, CH), 126.8 (CH), 126.5 (CH), 126.2 (J_{CPt} = 30 Hz, CH), 125.8 (CH), 125.4 (CH), 125.1 (CH), 125.0 (CH), 124.8 (CH), 123.1 (CH), 122.3 (CH), 122.2 (CH), 122.0 (CH), 121.3 (J_{CPt} = 18 Hz, CH), 120.6 (CH), 47.0 (C), 27.2 (CH_3). Elemental analysis calcd for $C_{43}H_{32}F_3N_3O_3PtS$: C, 55.96; H, 3.49; N, 4.55; S, 3.47; found: C, 56.00; H, 3.66; N, 4.43; S, 3.65.

***mer*-3b.** Pale yellow solid. Yield: 75%. ^1H NMR (300.1 MHz, CD_2Cl_2): δ 8.32 (d, J_{HH} = 8.1 Hz, 1H), 8.28–7.97 (m, 9H), 7.94 (s, 1H), 7.64 (d with satellites, J_{HH} = 6.0 Hz, J_{HPt} = 30 Hz, 1H), 7.50–7.05 (m, 16H), 6.84 (s with satellites, J_{HPt} = 15 Hz, 1H), 6.56 (s with satellites, J_{HPt} = 32 Hz, 1H), 1.66 (s, 3H), 1.60 (s, 3H), 1.57 (s, 6H), 1.48 (s, 6H). $^{13}C\{^1H\}$ NMR (75.45 MHz, CD_2Cl_2): δ 168.1 (C), 166.1 (C), 164.7 (C), 161.9 (C), 160.6 (C), 155.1 (C), 155.0 (C), 152.4 (C), 151.2 (C), 150.3 (CH), 148.8 (CH), 146.2 (CH), 144.0 (C), 143.7 (C), 142.5 (C), 141.6 (CH), 141.4 (CH), 140.5 (CH), 138.6 (C), 138.4 (C), 138.2 (C), 137.9 (C), 129.1 (CH), 128.9 (CH), 128.6 (CH), 127.4 (CH), 127.3 (CH), 125.0 (CH), 124.8 (CH), 124.5 (CH), 123.2 (CH), 123.1 (CH), 122.2 (CH), 122.1 (CH), 122.0 (CH), 121.6 (CH), 121.2 (CH), 121.1 (CH), 121.0 (CH), 120.8 (CH), 120.5 (CH), 118.3 (J_{CPt} = 31 Hz, CH), 47.1 (C), 47.1 (C), 47.0 (C), 27.8 (CH_3), 27.3 (CH_3), 27.2 (CH_3), 27.2 (CH_3), 26.9 (CH_3). Elemental analysis calcd for $C_{61}H_{48}F_3N_3O_3PtS$: C, 63.42; H, 4.19; N, 3.64; S, 2.78; found: C, 63.22; H, 4.29; N, 3.44; S, 2.95.

Synthesis of *fac*-[Pt(C^N)$_2$(flpy)]OTf

A degassed solution of *mer*-**3ab** or *mer*-**3b** (0.15 mmol) in MeCN (350 mL) was irradiated in a UV photoreactor for 3 h. The solvent was evaporated under reduced pressure and the remaining residue was chromatographed on silica gel using a $CHCl_3$/MeOH mixture in a 6 : 1 (***fac*-3ab**) or 9 : 1 (***fac*-3b**) ratio as the eluent.

***fac*-3ab.** White solid. Yield: 24%. ^1H NMR (400.9 MHz, CD_3CN): δ 8.39 (d, J_{HH} = 8.3 Hz, 1H), 8.29 (d, J_{HH} = 8.0 Hz, 2H), 8.15–8.09 (m, 4H), 8.00–7.94 (m, 2H), 7.78 (d with satellites, J_{HH} = 5.1 Hz, J_{HPt} ~9 Hz, 1H), 7.73 (d with satellites, J_{HH} = 5.2 Hz, J_{HPt} ~9 Hz, 2H), 7.51 (d, J_{HH} = 7.6 Hz, 1H), 7.39–7.12 (m, 9H), 7.06 (m, 1H), 6.89 (s with satellites, J_{HPt} = 47 Hz, 1H), 6.66 (dd with satellites, J_{HH} = 5.5, 0.9 Hz, J_{HPt} = 45 Hz, 1H), 6.64 (dd with satellites, J_{HH} = 5.5, 0.8 Hz, J_{HPt} = 45 Hz, 1H), 1.57 (s, 3H), 1.47 (s, 3H). $^{13}C\{^1H\}$ NMR (100.9 MHz, CD_3CN): δ 163.5 (C), 163.4 (C), 163.3 (C), 156.0 (C), 152.9 (C), 148.3 (CH), 148.2 (CH), 144.2 (C), 143.0 (C), 142.8 (C), 142.7 (CH), 142.6 (CH), 141.9 (C), 141.3 (C), 139.0 (C), 133.7 (J_{CPt} = 58 Hz, CH), 133.5 (J_{CPt} = 58 Hz, CH), 132.9 (J_{CPt} = 50 Hz, CH), 129.8 (CH), 128.6 (CH), 127.5 (CH), 127.5 (CH), 127.4 (CH), 126.7 (CH), 126.7 (CH), 126.2 (J_{CPt} = 10 Hz, CH), 124.3 (CH), 123.8 (J_{CPt} = 51 Hz, CH), 123.1 (CH), 123.0 (CH), 122.8 (CH), 122.0 (J_{CPt} = 35 Hz, CH), 121.4 (CH), 47.9 (C), 27.6 (CH_3), 27.5 (CH_3). Elemental analysis calcd for $C_{43}H_{32}F_3N_3O_3PtS$: C, 55.96; H, 3.49; N, 4.55; S, 3.47; found: C, 56.06; H, 3.56; N, 4.78; S, 3.23.

***fac*-3b.** Beige solid. Yield: 27%. ^1H NMR (400.9 MHz, CD_2Cl_2): δ 8.26 (d, J_{HH} = 8.2 Hz, 3H), 8.08 (td, J_{HH} = 7.8, 0.8 Hz,

3H), 7.95 (s, 3H), 7.71 (d with satellites, J_{HH} = 5.2 Hz, J_{HPt} ~9 Hz, 3H), 7.45 (d, J_{HH} = 7.6 Hz, 3H), 7.35 (td, J_{HH} = 6.5, 0.8 Hz, 3H), 7.27 (d, J_{HH} = 7.2, 1.2 Hz, 3H), 7.17–7.09 (m, 6H), 7.04 (s with satellites, J_{HPt} = 57 Hz, 3H), 1.63 (s, 9H), 1.51 (s, 9H). $^{13}C\{^1H\}$ NMR (75.45 MHz, CD_2Cl_2): δ 163.0 (C), 154.9 (C), 151.9 (C), 146.7 (CH), 143.7 (C), 141.4 (C), 141.1 (CH), 139.8 (C), 138.2 (C), 128.6 (CH), 127.3 (CH), 125.0 (CH), 123.7 (J_{CPt} = 50 Hz, CH), 123.0 (CH), 121.6 (J_{CPt} = 15 Hz, CH), 120.9 (CH), 120.5 (J_{CPt} = 35 Hz, CH), 47.0 (C), 27.8 (CH_3), 26.9 (CH_3). Elemental analysis calcd for $C_{61}H_{48}F_3N_3O_3PtS$: C, 63.42; H, 4.19; N, 3.64; S, 2.78.

Computational methods

DFT calculations were carried out with the Gaussian 09 package,[32] using the B3LYP hybrid functional,[33] together with the 6-31G**[34] basis set for the main-group elements and the LANL2DZ[35] basis set and effective core potential for the platinum atom. Geometry optimizations were carried out without symmetry restrictions, using "tight" convergence criteria and "ultrafine" integration grid. Vertical excitation energies were obtained from TDDFT calculations at the ground-state optimized geometries. Triplet-state geometry optimizations were carried out following a two-step strategy.[36] Initially, TDDFT optimizations of the two lowest triplets were attempted starting from the ground-state geometry; the resulting lowest-energy geometry was then subjected to spin-unrestricted DFT (UB3LYP) optimizations setting a triplet multiplicity. The solvent effect (CH_2Cl_2) was accounted for in all cases by using the integral equation formalism variant of the polarizable continuum solvation model (IEFPCM).[37] All geometry optimizations were followed by vibrational frequency calculations to verify that the obtained structures are minima on the potential energy surface. Natural spin densities were obtained from natural population analyses using the NBO 5.9 program.[38]

Acknowledgements

This work was supported by Ministerio de Economía y Competitividad, Spain (grant CTQ2015-69568-P), Ministerio de Educación, Cultura y Deporte, Spain (FPU grant to F. J.), Fundación Séneca (grant 19890/GERM/15) and Universidad de Murcia.

Notes and references

1 V. Balzani, G. Bergamini and P. Ceroni, *Angew. Chem., Int. Ed.*, 2015, **54**, 11320.
2 H. Yersin, A. F. Rausch, R. Czerwieniec, T. Hofbeck and T. Fischer, *Coord. Chem. Rev.*, 2011, **255**, 2622.
3 (*a*) E. Baggaley, J. A. Weinstein and J. A. G. Williams, *Coord. Chem. Rev.*, 2012, **256**, 1762; (*b*) Q. Zhao, C. Huang and F. Li, *Chem. Soc. Rev.*, 2011, **40**, 2508; (*c*) E. Baggaley, S. W. Botchway, J. W. Haycock, H. Morris, I. V. Sazanovich, J. A. G. Williams and J. A. Weinstein, *Chem. Sci.*, 2014, **5**, 879; (*d*) D.-L. Ma, V. P.-Y. Ma, D. S.-H. Chan, K.-H. Leung, H.-Z. He and C.-H. Leung, *Coord. Chem. Rev.*, 2012, **256**, 3087.
4 (*a*) C. K. Prier, D. A. Rankic and D. W. C. MacMillan, *Chem. Rev.*, 2013, **113**, 5322; (*b*) J. M. R. Narayanam and C. R. J. Stephenson, *Chem. Soc. Rev.*, 2011, **40**, 102; (*c*) D. M. Schultz and T. P. Yoon, *Science*, 2014, 343; (*d*) A. Inagaki and M. Akita, *Coord. Chem. Rev.*, 2010, **254**, 1220.
5 (*a*) A. Ruggi, F. W. B. van Leeuwen and A. H. Velders, *Coord. Chem. Rev.*, 2011, **255**, 2542; (*b*) R. Lincoln, L. Kohler, S. Monro, H. Yin, M. Stephenson, R. Zong, A. Chouai, C. Dorsey, R. Hennigar, R. P. Thummel and S. A. McFarland, *J. Am. Chem. Soc.*, 2013, **135**, 17161.
6 (*a*) J. Kalinowski, V. Fattori, M. Cocchi and J. A. G. Williams, *Coord. Chem. Rev.*, 2011, **255**, 2401; (*b*) W.-Y. Wong and C.-L. Ho, *J. Mater. Chem.*, 2009, **19**, 4457; (*c*) R. D. Costa, E. Ortí, H. J. Bolink, F. Monti, G. Accorsi and N. Armaroli, *Angew. Chem., Int. Ed.*, 2012, **51**, 8178.
7 (*a*) A. Juris, V. Balzani, F. Barigelletti, S. Campagna, P. Belser and A. von Zelewsky, *Coord. Chem. Rev.*, 1988, **84**, 85; (*b*) J. V. Caspar and T. J. Meyer, *Inorg. Chem.*, 1983, **22**, 2444; (*c*) D. S. Tyson, C. R. Luman, X. Zhou and F. N. Castellano, *Inorg. Chem.*, 2001, **40**, 4063; (*d*) Y.-Q. Fang, N. J. Taylor, G. S. Hanan, F. Loiseau, R. Passalacqua, S. Campagna, H. Nierengarten and A. V. Dorsselaer, *J. Am. Chem. Soc.*, 2002, **124**, 7912.
8 (*a*) Y. You and S. Y. Park, *Dalton Trans.*, 2009, 1267; (*b*) Y. You and W. Nam, *Chem. Soc. Rev.*, 2012, **41**, 7061; (*c*) A. B. Tamayo, B. D. Alleyne, P. I. Djurovich, S. Lamansky, I. Tsyba, N. N. Ho, R. Bau and M. E. Thompson, *J. Am. Chem. Soc.*, 2003, **125**, 7377; (*d*) B. J. Coe, M. Helliwell, S. Sánchez, M. K. Peers and N. S. Scrutton, *Dalton Trans.*, 2015, **44**, 15420.
9 (*a*) K. Li, G. S. Ming Tong, Q. Wan, G. Cheng, W.-Y. Tong, W.-H. Ang, W.-L. Kwong and C.-M. Che, *Chem. Sci.*, 2016, **7**, 1653; (*b*) J. A. G. Williams, S. Develay, D. L. Rochester and L. Murphy, *Coord. Chem. Rev.*, 2008, **252**, 2596; (*c*) R. McGuire Jr., M. C. McGuire and D. R. McMillin, *Coord. Chem. Rev.*, 2010, **254**, 2574.
10 J. Li, P. I. Djurovich, B. D. Alleyne, M. Yousufuddin, N. N. Ho, J. C. Thomas, J. C. Peters, R. Bau and M. E. Thompson, *Inorg. Chem.*, 2005, **44**, 1713.
11 (*a*) T. Sajoto, P. I. Djurovich, A. B. Tamayo, J. Oxgaard, W. A. Goddard and M. E. Thompson, *J. Am. Chem. Soc.*, 2009, **131**, 9813; (*b*) J. V. Caspar and T. J. Meyer, *J. Am. Chem. Soc.*, 1983, **105**, 5583.
12 (*a*) C. Bronner and O. S. Wenger, *Dalton Trans.*, 2011, **40**, 12409; (*b*) M. La Deda, A. Crispini, I. Aiello, M. Ghedini, M. Amati, S. Belviso and F. Lelj, *Dalton Trans.*, 2011, **40**, 5259.
13 (*a*) T. S. Teets and D. G. Nocera, *J. Am. Chem. Soc.*, 2009, **131**, 7411; (*b*) N. J. Farrer, J. A. Woods, L. Salassa, Y. Zhao, K. S. Robinson, G. Clarkson, F. S. Mackay and P. J. Sadler, *Angew. Chem., Int. Ed.*, 2010, **49**, 8905.

14 C.-F. Chang, Y.-M. Cheng, Y. Chi, Y.-C. Chiu, C.-C. Lin, G.-H. Lee, P.-T. Chou, C.-C. Chen, C.-H. Chang and C.-C. Wu, *Angew. Chem., Int. Ed.*, 2008, **47**, 4542.
15 (*a*) J. A. G. Williams, A. Beeby, E. S. Davies, J. A. Weinstein and C. Wilson, *Inorg. Chem.*, 2003, **42**, 8609; (*b*) D. Ravindranathan, D. A. K. Vezzu, L. Bartolotti, P. D. Boyle and S. Huo, *Inorg. Chem.*, 2010, **49**, 8922.
16 (*a*) D. A. K. Vezzu, J. C. Deaton, J. S. Jones, L. Bartolotti, C. F. Harris, A. P. Marchetti, M. Kondakova, R. D. Pike and S. Huo, *Inorg. Chem.*, 2010, **49**, 5107; (*b*) P.-K. Chow, G. Cheng, G. S. M. Tong, W.-P. To, W.-L. Kwong, K.-H. Low, C.-C. Kwok, C. Ma and C.-M. Che, *Angew. Chem., Int. Ed.*, 2015, **54**, 2084.
17 S.-C. Lo, R. E. Harding, C. P. Shipley, S. G. Stevenson, P. L. Burn and I. D. W. Samuel, *J. Am. Chem. Soc.*, 2009, **131**, 16681.
18 (*a*) G. F. Strouse, J. R. Schoonover, R. Duesing, S. Boyde, W. E. Jones Jr. and T. J. Meyer, *Inorg. Chem.*, 1995, **34**, 473; (*b*) S. C. F. Kui, I. H. T. Sham, C. C. C. Cheung, C.-W. Ma, B. Yan, N. Zhu, C.-M. Che and W.-F. Fu, *Chem. – Eur. J.*, 2007, **13**, 417.
19 T. Sajoto, P. I. Djurovich, A. Tamayo, M. Yousufuddin, R. Bau, M. E. Thompson, R. J. Holmes and S. R. Forrest, *Inorg. Chem.*, 2005, **44**, 7992.
20 (*a*) M.-Y. Yuen, S. C. F. Kui, K.-H. Low, C.-C. Kwok, S. S.-Y. Chui, C.-W. Ma, N. Zhu and C.-M. Che, *Chem. – Eur. J.*, 2010, **16**, 14131; (*b*) S. C. F. Kui, F.-F. Hung, S.-L. Lai, M.-Y. Yuen, C.-C. Kwok, K.-H. Low, S. S.-Y. Chui and C.-M. Che, *Chem. – Eur. J.*, 2012, **18**, 96.
21 P. K. Chow, C. Ma, W.-P. To, G. S. M. Tong, S.-L. Lai, S. C. F. Kui, W.-M. Kwok and C.-M. Che, *Angew. Chem., Int. Ed.*, 2013, **52**, 11775.
22 (*a*) W.-P. To, K. T. Chan, G. S. M. Tong, C. Ma, W.-M. Kwok, X. Guan, K.-H. Low and C.-M. Che, *Angew. Chem., Int. Ed.*, 2013, **52**, 6648; (*b*) G. Cheng, K. T. Chan, W.-P. To and C.-M. Che, *Adv. Mater.*, 2014, **26**, 2540.
23 F. Juliá, D. Bautista, J. M. Fernández-Hernández and P. González-Herrero, *Chem. Sci.*, 2014, **5**, 1875.
24 F. Juliá, G. Aullón, D. Bautista and P. González-Herrero, *Chem. – Eur. J.*, 2014, **20**, 17346.
25 F. Juliá, D. Bautista and P. González-Herrero, *Chem. Commun.*, 2016, **52**, 1657.
26 D. M. Jenkins and S. Bernhard, *Inorg. Chem.*, 2010, **49**, 11297.
27 J.-Y. Cho, K. Y. Suponitsky, J. Li, T. V. Timofeeva, S. Barlow and S. R. Marder, *J. Organomet. Chem.*, 2005, **690**, 4090.
28 A. F. Rausch, L. Murphy, J. A. G. Williams and H. Yersin, *Inorg. Chem.*, 2012, **51**, 312.
29 C. P. Newman, K. Casey-Green, G. J. Clarkson, G. W. V. Cave, W. Errington and J. P. Rourke, *Dalton Trans.*, 2007, 3170.
30 A. Tsuboyama, H. Iwawaki, M. Furugori, T. Mukaide, J. Kamatani, S. Igawa, T. Moriyama, S. Miura, T. Takiguchi, S. Okada, M. Hoshino and K. Ueno, *J. Am. Chem. Soc.*, 2003, **125**, 12971.
31 D. C. Powers, D. Benitez, E. Tkatchouk, W. A. Goddard and T. Ritter, *J. Am. Chem. Soc.*, 2010, **132**, 14092.
32 M. J. Frisch, G. W. Trucks, H. B. Schlegel, G. E. Scuseria, M. A. Robb, J. R. Cheeseman, G. Scalmani, V. Barone, B. Mennucci, G. A. Petersson, H. Nakatsuji, M. Caricato, X. Li, H. P. Hratchian, A. F. Izmaylov, J. Bloino, G. Zheng, J. L. Sonnenberg, M. Hada, M. Ehara, K. Toyota, R. Fukuda, J. Hasegawa, M. Ishida, T. Nakajima, Y. Honda, O. Kitao, H. Nakai, T. Vreven, J. A. Montgomery Jr., J. E. Peralta, F. Ogliaro, M. Bearpark, J. J. Heyd, E. Brothers, K. N. Kudin, V. N. Staroverov, R. Kobayashi, J. Normand, K. Raghavachari, A. Rendell, J. C. Burant, S. S. Iyengar, J. Tomasi, M. Cossi, N. Rega, N. J. Millam, M. Klene, J. E. Knox, J. B. Cross, V. Bakken, C. Adamo, J. Jaramillo, R. Gomperts, R. E. Stratmann, O. Yazyev, A. J. Austin, R. Cammi, C. Pomelli, J. W. Ochterski, R. L. Martin, K. Morokuma, V. G. Zakrzewski, G. A. Voth, P. Salvador, J. J. Dannenberg, S. Dapprich, A. D. Daniels, Ö. Farkas, J. B. Foresman, J. V. Ortiz, J. Cioslowski and D. J. Fox, *Gaussian 09 (Revision A.02)*, Gaussian Inc., Wallingford CT, 2009.
33 (*a*) A. D. Becke, *J. Chem. Phys.*, 1993, **98**, 5648; (*b*) C. T. Lee, W. T. Yang and R. G. Parr, *Phys. Rev. B: Condens. Matter*, 1988, **37**, 785.
34 (*a*) P. C. Hariharan and J. A. Pople, *Theor. Chim. Acta*, 1973, **28**, 213; (*b*) M. M. Francl, W. J. Pietro, W. J. Hehre, J. S. Binkley, M. S. Gordon, D. J. Defrees and J. A. Pople, *J. Chem. Phys.*, 1982, **77**, 3654.
35 P. J. Hay and W. R. Wadt, *J. Chem. Phys.*, 1985, **82**, 299.
36 D. Escudero and W. Thiel, *Inorg. Chem.*, 2014, **53**, 11015.
37 J. Tomasi, B. Mennucci and R. Cammi, *Chem. Rev.*, 2005, **105**, 2999.
38 E. D. Glendening, J. K. Badenhoop, A. E. Reed, J. E. Carpenter, J. A. Bohmann, C. M. Morales and F. Weinhold, *NBO 5.9*, Theoretical Chemistry Institute, University of Wisconsin, Madison, WI, 2009.
39 C. M. Cardona, W. Li, A. E. Kaifer, D. Stockdale and G. C. Bazan, *Adv. Mater.*, 2011, **23**, 2367.